

## Convoy Electrons Emitted from Resonant Coherently Excited Ions

K. Kimura,<sup>(a)</sup> J. P. Gibbons, S. B. Elston, C. Biedermann, R. DeSerio, N. Keller, J. C. Levin, M. Breinig, J. Burgdörfer, and I. A. Sellin

*Department of Physics, University of Tennessee, Knoxville, Tennessee 37996-1200  
and Oak Ridge National Laboratory, Oak Ridge, Tennessee 37831-6377*

(Received 27 July 1990)

We demonstrate the use of selective excitation of fast ions by resonant coherent excitation as a new technique to study convoy electron production. It is shown that electron loss from excited states plays an important role in convoy electron production by fast-channeled ions. The absolute cross section for convoy production by hydrogenic ions in  $n=2$  states is derived from the data, as is an estimate of the absolute probability of resonant coherent excitation as a function of ion energy.

PACS numbers: 34.90.+q, 61.80.Mk, 79.20.Nc

An axially channeled ion feels the anharmonic periodic potential of the crystal as an oscillatory electric field with a fundamental frequency  $\nu=v/d$ , where  $d$  is the atomic spacing along the axis and  $v$  is the ion velocity. When the frequency (or one of its higher harmonics) coincides with the excitation energy of the ion, resonant coherent excitation (RCE) can occur.<sup>1</sup> This effect has been observed through the change in the charge-state distribution of emergent ions<sup>2</sup> and, more recently, in the enhancement of projectile photon emission.<sup>3</sup> Thus RCE can now be used as a tool to selectively excite fast ions in solids. This technique, unlike laser pumping, has the advantage that any large excitation energy can be achieved by tuning the ion velocity. In the present work we report the first use of this technique to study convoy electron (CE) production by channeled ions. The production of CEs ejected in ion-solid collisions with electron velocity  $v_e$  very close to the ion velocity  $v$  has been intensively studied. It is now widely accepted that either electron loss to continuum<sup>4</sup> (ELC) or electron capture to continuum<sup>5</sup> (ECC) contribute to the production of CEs depending on the experimental conditions.<sup>6</sup>

Under channeling conditions, the ELC process is dominant because the electron capture probability, and thus the ECC probability, is drastically reduced.<sup>7</sup> In the ELC process, the important role of the excited states has been suggested.<sup>8-10</sup> Here we directly demonstrate the role of the excited states in CE production by changing the population of the excited states with RCE.

A beam of  $C^{5+}$  ions from the EN tandem accelerator at Oak Ridge National Laboratory was collimated by apertures to  $0.3 \times 0.3 \text{ mm}^2$  and to a divergence angle less than 0.4 mrad. A gold (100) single-crystal foil ( $\sim 160 \text{ nm}$  thick) was mounted on a two-axis goniometer and placed at the entrance focus of an electrostatic spherical sector spectrometer ( $\delta E/E \approx 0.01$ ). The electrons emitted into a forward cone of half-angle  $\theta_0 = 4.05^\circ$  were energy analyzed and detected by a microchannel plate (MCP).

Carbon ions emerging from the crystal passed through

an opening in the outer sector of the spectrometer and were collimated by an aperture behind the spectrometer. The acceptance half-angle of the aperture was 1.8 mrad, which is about  $\frac{1}{7}$  of the critical angle for  $\langle 100 \rangle$  channeling of 20-MeV  $C^{5+}$  ions. Thus, only well-channeled ions passing through the aperture were resolved into their charge states by an electrostatic analyzer and detected by a multidynode detector. Coincidences between CEs and emergent ions of charge state  $q_e$  were registered by a time-to-amplitude converter (TAC).

Figure 1 shows the energy dependence of the exit charge-state distributions for  $\langle 100 \rangle$ -aligned and random incidences of  $C^{5+}$  ions. While the charge-state distribution for random incidence changes monotonically, the distribution for  $\langle 100 \rangle$  channeled ions shows the effect of RCE, an enhancement of the  $C^{6+}$  fraction, around the

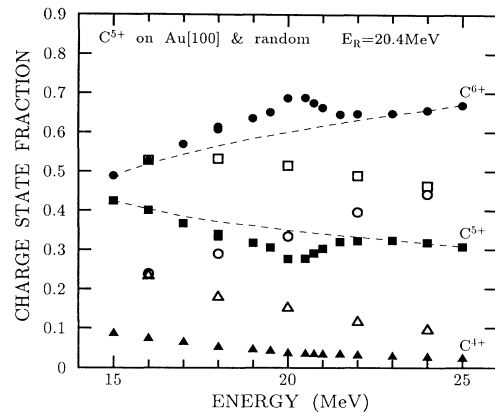


FIG. 1. Energy dependence of charge-state distribution of C ions transmitted through a gold crystal. Fractions of  $C^{4+}$  ( $\blacktriangle$ ),  $C^{5+}$  ( $\blacksquare$ ), and  $C^{6+}$  ions ( $\bullet$ ) for  $\langle 100 \rangle$ -aligned incidence of  $C^{5+}$  ions, and fractions of  $C^{4+}$  ( $\triangle$ ),  $C^{5+}$  ( $\square$ ), and  $C^{6+}$  ions ( $\circ$ ) for random incidence of  $C^{5+}$  ions are shown. Enhancement of the  $C^{6+}$  fraction is seen near the energy of resonant coherent excitation (20.4 MeV). Dashed lines estimate the fractions without the effect of RCE, and are drawn to guide the eye.

calculated resonance energy  $E_R$  (20.4 MeV, second harmonic for  $n=1$  to  $n=2$ ). This enhancement is explained by the differentially high electron-loss probability of the excited  $C^{5+}$  ion produced by RCE.<sup>2</sup> The agreement between the present result and that of Moak *et al.*<sup>11</sup> is very good.

The velocity distributions of CEs observed in coincidence with ions of exit charge states  $q_e = 5, 6$  were measured for (100)-aligned incidence of  $C^{5+}$  ions. The shape of the distributions was almost independent of either the ion energy or the exit charge state. The velocity distribution, whose FWHM was about 0.5 a.u., was integrated between  $v \pm 0.5$  a.u. to obtain the yield of CEs in coincidence with exit  $C^{q_e+}$  ions,  $Y(q_e)$ . The detection efficiency of the MCP was estimated to be  $(60 \pm 20)\%$ .<sup>12</sup>

If the mean free path for projectile charge changing and the target thickness are much larger than the attenuation length  $\lambda$  for the CEs (true for the present case), the equilibrium yield of CEs accompanied by ions of exit charge state  $q_e$  can be written<sup>9</sup> as

$$Y(q_e) = \lambda n_a [N(q_e) \sigma_{\text{ECC}}^{q_e} + N_g(q_e - 1) \sigma_{\text{ELC}}^{q_e - 1, g} + N_{\text{ex}}(q_e - 1) \sigma_{\text{ELC}}^{q_e - 1, \text{ex}}], \quad (1)$$

where  $n_a$  is the atomic density of the solid,  $N(q_e)$  is the total number of exit ions of charge  $q_e$ ,  $N_{g, \text{ex}}(q_e - 1)$  is the number of exit ions of charge  $q_e - 1$  in ground and excited states, respectively,  $\sigma_{\text{ECC}}^{q_e}$  is the ECC cross section for ions of charge  $q_e$ , and  $\sigma_{\text{ELC}}^{q_e - 1, g, \text{ex}}$  is the ELC cross section for ions of charge  $q_e - 1$  in the ground and excited states, respectively. Several normalization methods were tried for the CE yield: (1) The normalization per incident ion,  $Y(q_e)/\sum_{q_e} N(q_e)$ , is a neutral normalization which does not focus on one particular production process. (2) If the ECC process is dominant,  $Y(q_e)/N(q_e)$  is appropriate and this normalized yield is proportional to the ECC cross section of the  $q_e$  ions.<sup>9</sup> (3) If the ELC process is dominant,  $Y(q_e)/N(q_e - 1)$  is appropriate and proportional to the effective ELC cross section of the  $q_e - 1$  ions.<sup>9</sup>

Figure 2 displays the energy dependence of the CE yield measured in coincidence with exit  $C^{6+}$  ions normalized in three different ways: (a)  $Y(6)/\sum N(q_e)$ , (b)  $Y(6)/N(6)$ , and (c)  $Y(6)/N(5)$ . While  $Y(6)/\sum N(q_e)$  decreases monotonically with increasing energy (to be explained later), other normalized yields show structures. There is a dip at  $E_R$  in Fig. 2(b). As RCE cannot affect the ECC cross section of  $C^{6+}$  ions, this dip is ascribed to the inappropriate normalization, and is an artifact of the fact that  $N(6)$  is increased at  $E_R$  by ionization of excited  $C^{5+}$  ions. This confirms the fact that the contribution of the ECC process is small for fast-channeled ions. The peak at  $E_R$  in Fig. 2(c) shows an enhancement of the electron-loss cross section of  $C^{5+}$  ions due to RCE. For further discussion, it is necessary to consider the excited-state population of  $C^{5+}$  ions.

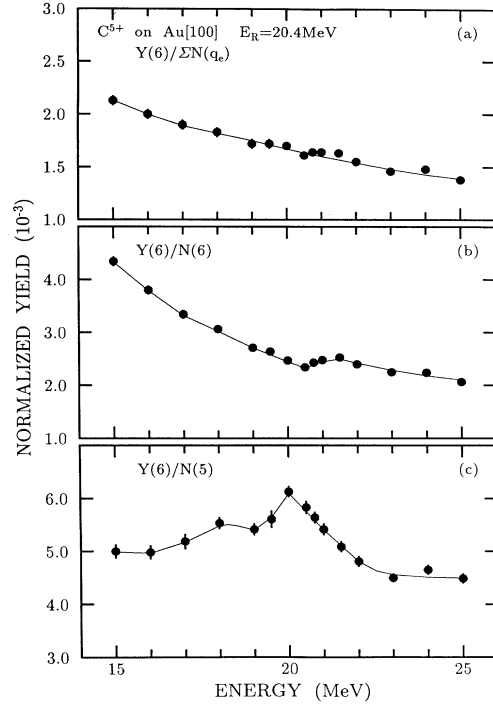


FIG. 2. Energy dependence of absolute CE yields measured in coincidence with exit  $C^{6+}$  ions for (100)-aligned incidence of  $C^{5+}$  normalized in three different ways (see text): (a)  $Y(6)/[N(4)+N(5)+N(6)]$ , (b)  $Y(6)/N(6)$ , and (c)  $Y(6)/N(5)$ . Only the relative errors are shown; the error in the MCP efficiency is not included. Lines are drawn to guide the eye.

We can estimate the fractions of  $C^{5+}$  ions in ( $nl$ ) states,  $F_{nl}^{5+}$ , using the observed charge-state distributions. When an ion travels through a crystal channel, the ion interacts only with loosely bound target electrons. If the ion velocity  $v$  is much faster than the Fermi velocity of the target crystal, the penetrating ion may be viewed in its frame as being bombarded by a flux of electrons moving at velocity  $v$ . Since the electron-capture probability is drastically reduced for channeled ions, the evolution of  $F_{nl}^{5+}$  along the path of the ion through the crystal is approximately described considering only electron loss and excitation by electron impact

$$\begin{aligned} \frac{dF_{1s}^{5+}}{dx} &= -n_e (\sigma_{1s}^{5+} + \sigma_{1s-2s}^{5+} + \sigma_{1s-2p}^{5+}) F_{1s}^{5+}, \\ \frac{dF_{2s,2p}^{5+}}{dx} &= n_e (\sigma_{1s-2s,2p}^{5+} F_{1s}^{5+} - \sigma_{2s,2p}^{5+} F_{2s,2p}^{5+}), \end{aligned} \quad (2)$$

where  $\sigma_{nl}^{5+}$  and  $\sigma_{1s-nl}^{5+}$  are ionization and excitation cross sections of  $C^{5+}$  ions by electron impact; we have used values given in the literature.<sup>13</sup> We neglected deexcitation because the excited-state ionization cross sections are much larger than the deexcitation cross sections.<sup>13</sup> We also neglect the excited states  $n \geq 3$ , because the electrons in these excited states have orbital radii compa-

table to or larger than the radius of the crystal channel. Even though this approximation is crude, the basic features of the evolution of  $F_{nl}^{5+}$  are well described by Eq. (2). The solution to Eq. (2) with the initial condition  $F_{1s}^{5+} = 1$  is

$$F_{1s}^{5+} = \exp[-n_e x (\sigma_{1s}^{5+} + \sigma_{1s-2s}^{5+} + \sigma_{1s-2p}^{5+})],$$

$$F_{2s,2p}^{5+} = \frac{\sigma_{1s-2s,2p}^{5+}}{\sigma_{1s}^{5+} + \sigma_{1s-2s}^{5+} + \sigma_{1s-2p}^{5+} - \sigma_{2s,2p}^{5+}} \{ \exp(-n_e x \sigma_{2s,2p}^{5+}) - \exp[-n_e x (\sigma_{1s}^{5+} + \sigma_{1s-2s}^{5+} + \sigma_{1s-2p}^{5+})] \}.$$

The unknown parameter  $n_e$  can be determined by comparing the calculated  $C^{5+}$  fraction,  $F^{5+} = F_{1s}^{5+} + F_{2s}^{5+} + F_{2p}^{5+}$ , with the experimental one. Because Eq. (2) does not contain the effect of RCE, the calculation must be compared with the experimental result shown by dashed lines in Fig. 1 (which estimate the charge-state distribution without the effect of the RCE). The electron density obtained at 20 MeV,  $n_e = 3.2 \times 10^{23} \text{ cm}^{-3}$ , agrees very well (within 20%) with the electron density in the channel center calculated with a Molière potential. The effect of RCE can then be taken into account by substituting  $\sigma_{1s-2p}^{5+} + P/n_e$  for  $\sigma_{1s-2p}^{5+}$ , where  $P$  is the probability of RCE per unit path length of the ion. This probability, determined here for the first time, can be obtained by comparing the calculated  $C^{5+}$  fraction with the observed result. Figure 3(a) shows this RCE probability as a function of the discrete ion energies measured.  $P$  has a peak at an energy slightly lower than the calculated resonance energy (20.4 MeV) and has a tail on the low-energy side showing the Stark shift of the energy levels of an ion moving in the crystal channel due to the

wake potential and the crystal field.<sup>14</sup> The effective RCE cross section,  $P(E_R)/n_e = 8.8 \times 10^{-20} \text{ cm}^2$ , is about one-half of the excitation cross section by electron impact,  $\sigma_{1s-2p}^{5+} = 1.8 \times 10^{-19} \text{ cm}^2$ .

The RCE probability per unit path length can be also estimated from Fermi's "golden rule,"

$$P(E_R) = 2\pi F^2 |\langle 2p | z | 1s \rangle|^2 \rho(E_R) / \hbar v,$$

using the Fourier coefficient of the electric field in the channel center,  $F \approx 0.13 \text{ a.u.}$ ,<sup>11</sup> and the state density  $\rho(E_R) \approx 0.56 \text{ a.u.}^{-1}$  estimated from the shape of the peak in Fig. 3(a). The result,  $P(E_R) \sim 2.1 \mu\text{m}^{-1}$ , agrees reasonably with the experimental result,  $2.8 \mu\text{m}^{-1}$ . Using the  $n_e$  and  $P$  values obtained, the excited-state population of  $C^{5+}$  ions,  $F_{nl}^{5+}$ , can be calculated [Fig. 3(b)]. The  $n=2$  population of  $C^{5+}$  ions decreases monotonically with increasing energy, showing no apparent effect of RCE. The smooth energy dependence of the  $n=2$  population of  $C^{5+}$  is mainly due to the large ionization cross section of excited states as compared with the effective RCE cross section ( $\sigma_{2p}^{5+} = 7.4 \times 10^{-19} \text{ cm}^2$  and  $P/n_e = 8.8 \times 10^{-20} \text{ cm}^2$  at 20 MeV). In effect, the resonant excitation of  $2p$  states is compensated by the reduction in the population of  $C^{5+}$  ( $1s$ ) ions near the exit surface in such a way that the  $n=2$  population decreases nearly monotonically.

The effect of RCE is primarily seen as a dip at  $E_R$  in the ground-state population of  $C^{5+}$  ions. Therefore, the ratio of the population of the excited  $C^{5+}$  ions to that of the ground-state  $C^{5+}$  ions increases at  $E_R$ . This causes the enhancement of the effective ELC cross section seen in Fig. 2(c). Since  $P \propto |\langle 2p | z | 1s \rangle|^2 \propto Z^{-2}$  and the ionization cross section is proportional to  $Z^{-4}$ ,<sup>13</sup> where  $Z$  is the atomic number of the projectile, an observable enhancement of  $n=2$  population at resonance can be expected for heavier ions. In fact, a  $2p$  population enhancement has been observed<sup>3</sup> for higher- $Z$ -channeled projectiles ( $Z=9,12$ ) via resonantly enhanced Ly- $\alpha$  emission, which must be strictly proportional to the  $2p$  population.<sup>3</sup>

The fact that the energy dependence of the CE yield per incident ion [Fig. 2(a)] reflects that of the  $n=2$  population shown in Fig. 3(b) indicates that ELC from excited states dominates CE production under the present circumstances. We can estimate the ELC cross section by electron impact from the present results. Neglecting the first two terms in Eq. (1) and changing  $n_a$  to  $n_e$ , the

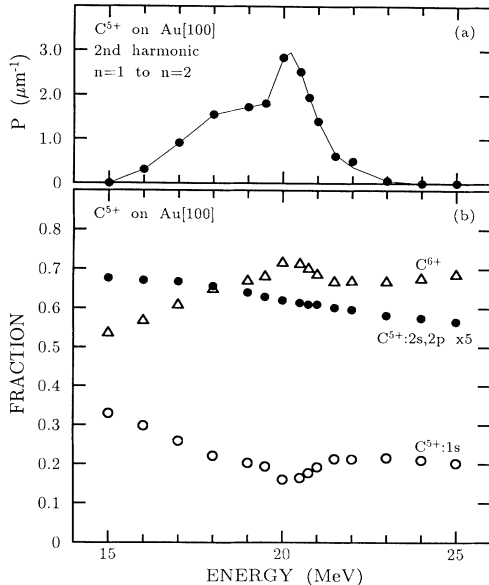


FIG. 3. (a) Probability of RCE per unit path length of  $C^{5+}$  ions in the Au  $\langle 100 \rangle$  channel, estimated from the observed charge-state distribution. The line is drawn to guide the eye. (b) Calculated  $C^{6+}$  fraction ( $\Delta$ ),  $1s$  state population ( $\circ$ ), and  $n=2$  state population ( $\bullet$ ) of  $C^{5+}$  ions as functions of energy.

CE yield can be written as  $Y(6) = \lambda n_e N_{\text{ex}}(5) \sigma_{\text{ELC}}^{5,\text{ex}}$ . Substituting  $\lambda = 1.4 \text{ nm}$ ,<sup>15</sup> and the present results into this equation we find the ELC cross section to be  $(3 \pm 1) \times 10^{-19} \text{ cm}^2$  at 20 MeV, or about 40% of the ionization cross section ( $\sigma_{2p}^{5+} = 7.4 \times 10^{-19} \text{ cm}^2$ ).<sup>13</sup> This ratio of the ELC cross section to the total ionization cross section is quite large as compared with binary ion-atom collisions. For example, the corresponding ratio is about 3% in the case of 20-MeV  $\text{O}^{7+}$  on Ar, where a much smaller fraction of the projectile ionization electrons were collected in a cone of half-angle  $\theta_0$  ( $\theta_0 = 1.8^\circ$  and  $\Delta v = 0.5 \text{ a.u.}$ ).<sup>4</sup> This suggests that electrons lost from excited states are strongly forward peaked and therefore have a large probability of becoming CEs as compared with those lost from the ground state, in line with a previous theoretical study.<sup>10</sup> In addition, the CE yield may also be increased by incoherently excited states for  $n \geq 3$ . As a check of the supposition implicit in the simple model underlying Eq. (2) that the probability of direct excitation to the continuum via RCE is small, we note that a third-harmonic resonance with  $n = 1$  to  $n = \infty$  occurs at 16.1 MeV for  $\text{C}^{5+}$  ions in Au  $\langle 100 \rangle$  channels. However, Fig. 2 does not show any anomaly of CE yield at that resonance energy, confirming that the probability of RCE to the continuum is small.

This work was supported by the National Science Foundation and by the U.S. Department of Energy under Contract No. DE-AC05-84OR21400 with Martin

Marietta Energy Systems, Inc.

<sup>(a)</sup>On leave from Department of Engineering Science, Kyoto University, Kyoto, Japan.

<sup>1</sup>V. V. Okorokov, Pis'ma Zh. Eksp. Teor. Fiz. **2**, 175 (1965) [JETP Lett. **2**, 111 (1965)].

<sup>2</sup>S. Datz *et al.*, Phys. Rev. Lett. **40**, 843 (1978).

<sup>3</sup>Y. Iwata *et al.*, Nucl. Instrum. Methods Phys. Res., Sect. B **48**, 163 (1990); S. Datz *et al.* (to be published).

<sup>4</sup>M. Breinig *et al.*, Phys. Rev. A **25**, 3015 (1982).

<sup>5</sup>K. Dettmann *et al.*, J. Phys. B. **7**, 269 (1974).

<sup>6</sup>Y. Yamazaki, Nucl. Instrum. Methods Phys. Res., Sect. B **48**, 97 (1990); J. Kemmler, *ibid.* **48**, 612 (1990).

<sup>7</sup>J. Kemmler (private communication).

<sup>8</sup>S. D. Berry *et al.*, J. Phys. B **19**, L149 (1986).

<sup>9</sup>H.-P. Hülskötter *et al.*, Phys. Rev. A **33**, 2156 (1986); H.-P. Hülskötter *et al.*, Nucl. Instrum. Methods Phys. Res., Sect. B **24/25**, 147 (1987).

<sup>10</sup>J. Burgdörfer *et al.*, Phys. Rev. A **28**, 3277 (1983).

<sup>11</sup>C. D. Moak *et al.*, Phys. Rev. A **19**, 977 (1979).

<sup>12</sup>M. Galanti *et al.*, Rev. Sci. Instrum. **42**, 1818 (1971); R. S. Gao *et al.*, *ibid.* **55**, 1756 (1984).

<sup>13</sup>L. B. Golden and D. H. Sampson, J. Phys. B **10**, 2229 (1977); Y. Itikawa *et al.*, At. Data **33**, 149 (1985).

<sup>14</sup>O. H. Crawford and R. H. Ritchie, Phys. Rev. A **20**, 1948 (1979).

<sup>15</sup>J. Burgdörfer and J. P. Gibbons, Phys. Rev. A **42**, 1206 (1990).